Theor Chem Acc (2006) 116: 338–346
DOI 10.1007/s00214-005-0072-2

REGULAR ARTICLE

Hui Xiong · Alejandro Crespo · Marcelo Marti
Dario Estrin · Adrian E. Roitberg

Free energy calculations with non-equilibrium methods: applications of the Jarzynski relationship

Received: 18 April 2005 / Accepted: 18 November 2005 / Published online: 6 January 2006

Abstract We present an introduction to the Jarzynski relationship that makes a strong connection, for a thermodynamic transformation, between the distribution of non-equilibrium work values and the corresponding equilibrium free energy differences. The relationship is discussed in the context of sampling issues, high level parallel computing and convergence criteria. We discuss three different applications by our group: mechanical unfolding of peptides, mixed quantum/classical free energy calculations in enzymes, and ligand escape pathways.

1 Introduction

Free energies are central quantities to both thermodynamics and kinetics, relating to experimentally determined properties such as equilibrium constants and reaction rates. Even though proper computation of enthalpies is relatively simple at particular molecular conformations, the estimate of the entropic factors requires sampling over large numbers of conformations obeying proper thermodynamic weights. This problem is by no means trivial, and it has been reviewed extensively over the years [1]. Modern applications of free energy calculations in computational chemistry include ligand binding [2], free energy profiles in mixed quantum–classical enzymatic calculations [3] and hydration [4]. These calculations are done under (if possible) equilibrium conditions, or with as full a sampling as possible.

H. Xiong · A. Crespo · A.E. Roitberg (✉)
Quantum Theory Project and Department of Physics,
University of Florida, P.O. Box 118435,
Gainesville, FL 32611-8435, USA
E-mail: roitberg@ufl.edu

A. Crespo · M. Marti · D. Estrin
Departamento de Química Inorgánica,
Analítica y Química-Física and INQUIMAE-CONICET,
Facultad de Ciencias Exactas y Naturales,
Universidad de Buenos Aires,
Ciudad Universitaria – Pab II, C1428EHA,
Buenos Aires, Argentina

In this article we review recent work done using non-equilibrium calculations of free energies, based on the so-called Jarzynski relationship (JR) [5–8] which has been extended and shown to be part of a subset of classical thermodynamics dealing with very small systems, as well as with fluctuations in macroscopic properties. In the 8 years since the original proposal by Jarzynski, a very large number of publications have appeared discussing derivations and re-derivations of the original theorem [5–27], analysis and suggestions for uses and improvements [10,16,28–38], experimental verifications [28,39–42] and a comparatively smaller number of direct applications of the technique [4,43–49]. The previous list is by no means complete, nor is the division into categories strict and well defined.

This article is structured as follows: first, we introduce the JR and discuss its connection to more classical methods for computation of free energies. We then present some of our recent results involving three different applications or the JR to biological systems, including some algorithmic comments related to error analysis and efficiency.

2 Free energy calculations

The Gibbs free energy difference between two states A and B is formally described by:

$$\Delta G_{\mathrm{A}\to\mathrm{B}} = -\Delta G_{\mathrm{B}\to\mathrm{A}} = G_{\mathrm{B}} - G_{\mathrm{A}} = -\frac{1}{\beta}\ln\left(\frac{Z_{\mathrm{B}}}{Z_{\mathrm{A}}}\right) = -\frac{1}{\beta}\ln\left(\frac{\int \mathrm{d}r\,\exp(-\beta H_{\mathrm{B}})}{\int \mathrm{d}r\,\exp(-\beta H_{\mathrm{A}})}\right) \quad (1)$$

where ΔG represents the Gibbs free energy difference, β is $1/k_{\mathrm{B}}T$ and Z stands for the canonical partition functions, which are explicitly written in terms of Boltzmann weights in the right-hand side of Eq. (1).

Computational methods for the calculation of such quantities have a long history. However, all of them have to surmount an important hurdle: in order to compute the partition function, very extensive (one might say complete) sampling of the phase space at both A and B must be done. This is of course unattainable except for the simplest systems, and one must rely on a number of approximations. One widely used idea can be traced to Zwanzig [50] and is known as free energy perturbation (FEP). It requires the calculation of the energy difference between states A and B, ensemble averaged over the initial ensemble A and is used as in:

$$\Delta G_{\mathrm{A}\to\mathrm{B}} = -\frac{1}{\beta}\ln\langle\exp(-\beta(H_{\mathrm{B}} - H_{\mathrm{A}}))\rangle_{\mathrm{A}} \tag{2}$$

The convergence of the exponential average is very slow, unless the two states are close in their phase-space coverage. Only conformations that have a low value of $H_{\mathrm{B}} - H_{\mathrm{A}}$ have a substantial weight in the average. This can be overcome by defining an intermediate system with no physical realization. van Gunsteren pioneered the use of single, unphysical reference states as a way to minimize the changes between initial and final ensembles [51,52].

One can also define a non-physical Hamiltonian that varies smoothly between A and B, as in:

$$H(\lambda) = H_0 + \lambda\,[(\,H_1 - H_0\,)]\,, \tag{3}$$

with $\lambda \in [0, 1]$. Other forms of the interpolation scheme can be used as long as the limiting cases for $\lambda \to 0$ $(H\,(0) = H_{\mathrm{A}})$ and $\lambda \to 1$ $(H\,(1) = H_{\mathrm{B}})$ are obeyed.

This interpolation can be used to compute the free energy difference of Eq. (2) as:

$$\Delta G_{0\to1} = -\frac{1}{\beta}\sum_{k=1}^{N-1}\ln\langle\exp\left(-\beta(H_{k+1} - H_k)\right)\rangle_k \tag{4}$$

Note that in this formulation, there is no need to directly compute the end-to-end enthalpy difference as in Eq. (2) highly increasing the convergence rate.

The definition of the λ-dependent Hamiltonian allows for the computation of free energy derivatives with respect to lambda, which in turns enables the calculation of the free energy difference between A and B using the so-called thermodynamics integration method (TI).

$$\Delta G_{0\to1} = \int_0^1 \mathrm{d}\lambda\left\langle\frac{\partial H(\lambda)}{\partial\lambda}\right\rangle_\lambda \tag{5}$$

If one thinks about the system as evolving from A to B with a time dependent Hamiltonian, then the above equations can be re-written simply by assuming a perturbation parameter, lambda as $\lambda = \lambda\,(t)$ (which obviously, according to Eq. (3), immediately means a Hamiltonian $H(t)$) and associated definition of work as in:

$$W(t) = \int_0^t \frac{\partial H(t)}{\partial t}\mathrm{d}t \tag{6}$$

The second law of thermodynamics requires that the ensemble average of the work done onto the system by an external perturbation (the change from A to B) be larger than or equal to the free energy difference, with the offset being the dissipative (non-useful) work.

$$\langle W_{\mathrm{A}\to\mathrm{B}}\rangle_{\mathrm{A}} \geq \Delta G_{\mathrm{A}\to\mathrm{B}} \tag{7}$$

The average is taken over different realizations of the transformation, each starting from a different conformation sampled from the equilibrium ensemble of state A. Under a quasi-static (QS) transformation from A to B (in infinite time), the perturbation is continuously very close to equilibrium conditions, and only then is the work exactly equal to the free energy difference. For true QS changes, all realizations of the experiment will give the same value of W, and a well defined value for ΔG. This is equivalent to the statement that the distribution of work values under a QS transformation is a delta function at the exact value of ΔG.

It is then clear than under non-QS changes from A to B, a number of statements must be true:

1. The average work will be larger than delta $G.\langle W\rangle > \Delta G$
2. The distribution of work values will have a finite width. $\sigma_W^2 > 0$.
3. Any individual realization could give rise to work values lower than ΔG. $\exists i / W_i < \Delta G$.

3 The original Jarzynski method

Even though these are interesting points, they were of only peripheral interest until a seminal article by Jarzynski in 1997 [5]. In that paper, he proved the so-called JR that states:

$$\begin{aligned}\Delta G_{A\to\mathrm{B}} &= -\frac{1}{\beta}\ln\langle\exp(-\beta W_{\mathrm{A}\to\mathrm{B}})\rangle_{\mathrm{A}}\\ &= -\frac{1}{\beta}\ln\sum_{i=1}^{N}\frac{1}{N}\exp(-\beta W_{i,\mathrm{A}\to\mathrm{B}})\end{aligned} \tag{8}$$

where W_i is the out of equilibrium work (for the ith realization) done onto the system when going from state A to state B, and the exponential average is done over an equilibrium ensemble for state A only. This formula seems very counterintuitive at first, since it makes a clear connection between non-equilibrium work values (which are, by definition, path dependent), with the equilibrium free energy, a state function (and hence not path dependent). Moreover, the only two requirements for this equality to work are that the initial ensemble over state A be equilibrated, and that the exponential average be converged, which in turns require a large number of realizations of the transformation. There is no requirement as to how the switch from state A to state B should be done (in a computational implementation: how fast can one switch the system's Hamiltonian from A to B).

First, let us see that this setup reduces to known expressions under certain limits. Clearly, if the switch is done infinitely slowly, then the transformation is QS. In that case, the work W is equal to the free energy (there is no dissipative work) and the JR is obviously true. In the other extreme, one could switch from state A to state B instantaneously. In that regime, the work done on the system is simply the enthalpy change between the initial and final points as in:

$$\Delta G_{A\rightarrow B} = -\frac{1}{\beta} \ln \langle \exp(-\beta(H_B - H_A)) \rangle_A \tag{9}$$

Note that this is simply FEP and that Eq. (9) is the same as the previously described Eq. (2).

In a general situation, the transformation of the system from A to B and the algorithmic application of the JR can be seen in Fig. 1. At an initial state A ($\lambda = 0$) the system is equilibrated. This is represented by the vertical line at left. This initial ensemble could be equilibrated by long molecular dynamics or Monte Carlo runs, or by advanced sampling techniques such as replica exchange [53]. Once this is done, a number N of initial snapshots are taken from the initial ensemble. They are then transformed into state B ($\lambda = 1$) (and all states in between) at a finite rate. The work for each realization is then computed, and the overall free energy is extracted by using the JR as shown in Eq. (8).

The demonstration of the validity of the JR is beyond the scope of this review, but the interested reader is encouraged to read the original article by Jarzynski [5]. However, it is important to provide a simple explanation of why this seemingly strange equality might work. Figure 2 gives a hint as to the behavior of the system. Under near-equilibrium conditions, the distribution of work values could be expected to be roughly Gaussian (this requirement is not needed, but makes explanations clearer). The vertical line at 0 unit of work (arbitrary units) represents the exact free energy difference in going from A to B. Under QS conditions, the distribution of work values is very nearly a delta function (a very narrow Gaussian). However, under any transformation rate larger than zero, two things happen at the same time. The average work gets larger as the rate increases while the width of the work distribution also increases. The JR requires a weighted average of this distribution with an exponential set

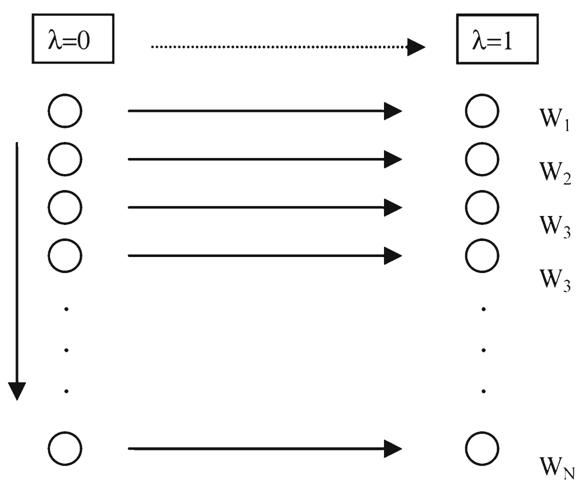

Fig. 1 Schematic view of the multiple steering mechanism used for this article

of weights. The net effect of this non-linear averaging is to pick, from the work distribution, trajectories that are low in work values. The number of these 'tail' trajectories of course decreases drastically with the transformation rate, and hence the effort required to converge the non-exponential average increases quickly. There is also a result seemingly contradicting the second law of thermodynamics: the probability of an individual realization of the transformation from A to B having work lower than the free energy difference between A and B is not zero. This would seem to indicate a negative dissipative work, which is of course not possible. An important point to remember is that the second law only applies to macroscopic systems (ensemble averages) and single realizations are 'allowed' to have low values of work. The proper quantity to compare to the free energy is the average work, which indeed is always larger than ΔG.

Given the exponential nature of the average, numerical convergence is an important issue. Early work of Hermans [29] has a remarkable connection to the JR. Hermans proposed, using fluctuation dissipation and linear response arguments, that if one performed many finite-time transformations starting from different initial conditions, one could improve on the simple linear average used until then, by making use of the standard deviation of the work calculations (or measured).

$$\Delta G \approx \langle W \rangle - \frac{\beta}{2}\sigma_W^2 \tag{10}$$

This relationship, which has been substantially used in the literature, turns out to be simply a cumulant expansion of Eq. (8). This could be shown in two ways, with an interesting relation to each other. First, if one assumes a Gaussian distribution of work values (a reasonable zeroth order approximation), then Eq. (10) is exact. If one describes the exponential average as a cumulant expansion, then Eq. (10) becomes simply the first and second order cumulants. There are also higher order cumulants (which are all exactly zero in the case of linear response), which alternate in sign and are very slowly converging.

The actual algorithmic advantage of the JR is not immediately obvious. Umbrella sampling or other methods could very well be as efficient in terms of computational requirements. The JR, by shifting the burden of equilibration to only the initial state, lifts the requirement for a slow, QS transformation. This is a perfect application for modern highly parallel, distributed computational systems. One should, in that environment, cease to discuss efficiency in terms of CPU time and instead focus on wall clock (return to user) time. Under these conditions, a trivially parallel JR application will finish in the time required for an individual pulling, with a very small overhead associated with data management and transmission. In this intrinsic parallelism resides the computational promise of the JR. Under conditions where a single (or a small number of CPUs) are available to the user, traditional methods are probably more appropriate. It is in the large number of CPUs available for short times that the JR becomes very useful.

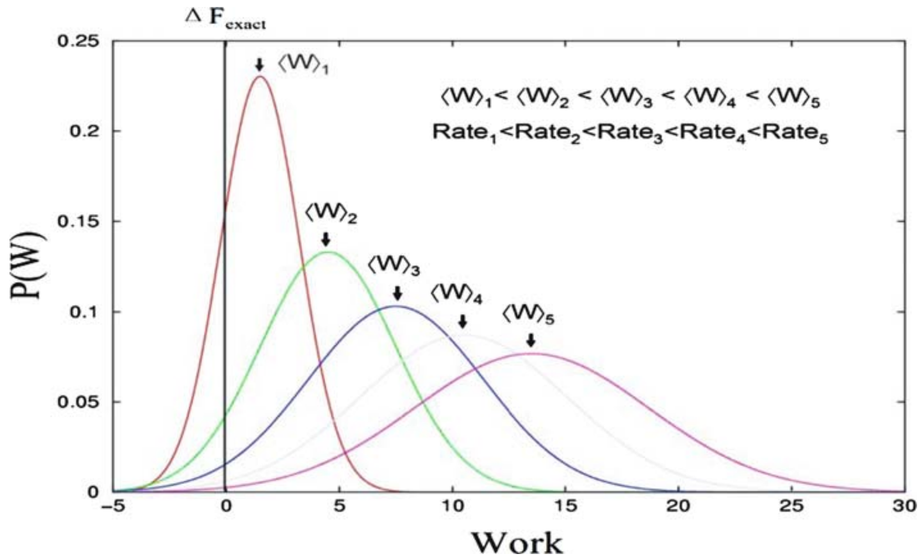

Fig. 2 Schematic work distributions for different switching rates

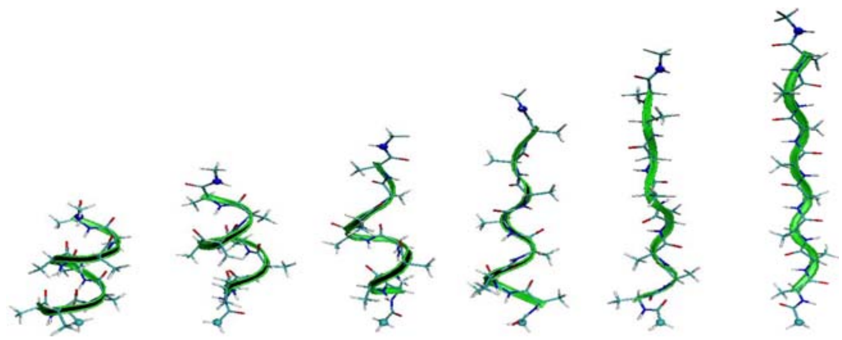

Fig. 3 Ace-Alanine8-NMe unfolded from α-helix to a fully-extended state by mechanical pulling

4 Three examples of the application of the JR

4.1 Mechanical stretching in biopolymers

In work to be submitted shortly to the Journal of Chemical Physics we use molecular dynamics to simulate unfolding of a simple Ace-Alanine$_8$-NMe peptide molecule by mechanical pulling (Fig. 3). The Free energy of pulling is calculated using the JR method and compared with conventional free energy calculation methods.

The Ace-Alanine$_8$-NMe peptide molecule is initially built in an all α-helical state. Two harmonic potentials are used: one attached to the Ace end with a force constant of 10,000 kcal/mol Å^{-2} is to effectively fix that end in space, and a force constant 100 kcal/mol Å^{-2} is used to restrain the N atom in the NMe residue at the other end. The distance in between is initially 13.2 Å. The simulation has been performed in vacuum (as a proof of principle of the method), without cutoffs for the non-bonded interactions. An initial equilibrium ensemble of configurations is generated by running molecular dynamics for 200 ns with both ends fixed, or, at pulling length 0.0 Å. As we will show later, the requirement of initial equilibration is stringent for a correct application of the JR. A number of published applications do not control this problem and might very well be flawed.

To pull the molecule, the second restraining potential is moved at a constant velocity. A (local) MPI implementation of the molecular dynamics program TINKER [54] is used on configurations drawn from an initially equilibrated ensemble to pull them into fully-extended states. Different pulling rates (1.0, 0.1, 0.01 and 0.001 Å/ps) are implemented to test Jarzynski's equality. The number of pulls was 20,000, 2,000, 200 and 20 for the different rates.

For comparison purpose the exact free energy curve is computed by pulling at an ultra slow rate (10^{-4} Å/ps). This free energy calculation method is conventionally known as "slow growth" (SG). The curve obtained is plotted in Fig. 4. The validity is confirmed by running multiple forward and reverse pullings, from which free energy curves are computed. All realizations superimpose in their work values, which guarantees reversibility.

Figure 5 shows the work distributions obtained for different pulling rates at different pulling lengths. The exact free energy curve of Fig. 4 is plotted in the "pulling length – work"

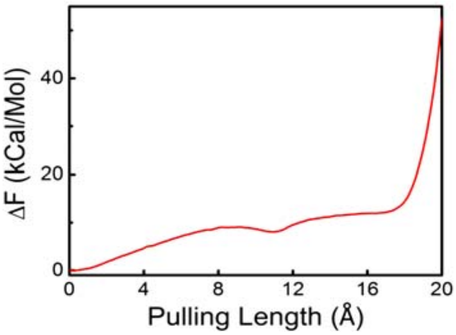

Fig. 4 Equilibrium free energy of pulling of Ace-Alanine8-NMe from α-helix to a fully-extended state

plane. From these distributions, work averages and free energy differences by JE are calculated and plotted in Fig. 6.

In accordance with Fig. 2, we see that the work distribution shifts and broadens as the pulling rate increases (more irreversibility). There is clearly sufficient sampling of the tail region in the two slowest rates (1 and 0.1 Å/ps), but the 0.01 Å/ps will probably fail when the distances exceed 6 Å.

In Fig. 6 we see that the JR estimate yield very good results when the pulling rate is slow or the pulling length is small. However, at larger pulling lengths, or for faster pullings, the work distribution moves away from the exact free energy difference. The total number of pullings will eventually become insufficient to yield correct free energy differences.

The JE method yields good convergence for slow pullings (0.001, 0.010, and 0.100 Å/ps) for a relatively small amount of total computing time, for which conventional FEP method fails to converge. It's not obvious that the JR method consumes less computing time than the SG method does. However, as described above, faster pulling rates allow for a faster return-to-user of the results by means of parallel computing.

4.2 QM/MM free energy calculations in enzymatic systems

We shall illustrate an application of the JR in the context of an efficient quantum-mechanical–molecular-mechanical (QM–MM) density functional theory (DFT) based scheme optimized for biomolecules. This section's results have been partly published elsewhere [55].

We study the conversion reaction of chorismate to prephenate, catalyzed by the *B. Subtilis* enzyme chorismate mutase, which has been extensively studied [56–62]. We have previously studied this system within the same setup as in the present article, using DFT and MM, computing activation energies [56].

Our QM–MM scheme uses, for the description of the QM region, a very efficient implementation DFT based on numerical basis sets called (Spanish initiative for electronic simulation of thousands of atoms SIESTA) [63].

The calculations have been performed employing a starting structure obtained from *B. subtilis* in the Protein Data Bank (1COM) [64] solvated with 496 TIP3P water molecules. The total system included the 24 substrate atoms (QM) plus 7115 MM atoms. The systems was equilibrated performing classical MD simulations using the Wang et al. [42] force field parametrization [65], as included in the Amber 7.0 package, taking both chorismate and prephenate as solutes.

From the last 2 ns of the classical simulation of chorismate and prephenate + chorismate mutase, we collected 20 starting structures of each (40 total), for our multiple steering QM–MM simulations. Each of these was relaxed at the QM–MM level for 0.5 ps at 300 K. The substrates moieties were treated QM at the DFT level and the rest of the system was treated at the MM level using the Wang et al. [42] force field parametrization.

Only atoms within a sphere of 15 Å from the QM structure were allowed to move. The reaction coordinate of this reaction, $\xi = d_{cc} - d_{co}$ has already been shown to represent adequately the process, and is shown in Fig. 7.

These 20+20 QM–MM relaxed structures were used as starting points for the multiple steering molecular dynamics (MSMD) runs. The reaction coordinate was changed from $\xi = 2.0$ Å to $\xi = -2.0$ Å for a set of 15+15 QM–MM structures at a constant speed of 2 Å/ps, and for another set of 5+5 QM–MM structures at a lower speed of 1 Å/ps. A force constant of 200 kcal/(molÅ) was used in all cases. For comparison, the potential of mean force was computed using an umbrella sampling scheme [66]. A total of 12 windows simulations of 5 ps each have been employed, using as starting structures the snapshots of the constrained energy minimizations performed previously.

All QM and QM–MM calculations have been performed using a DZVP basis sets, with a pseudoatomic orbital energy shift of 50 meV and the generalized gradient approximation of Perdew, Burke and Ernzerhof.

In Fig. 8a we show the values of accumulated work versus ξ for chorismate to prephenate conversion for the 20 repetitions. Also shown is the standard deviation of the work values. This data should be trusted from $\xi = 2$ Å to $\xi = -0.5$ Å, at which point $\sigma_w \geq 4k_B$T. Figure 8b has the same data starting at the prephenate side of the reaction. It is even clearer that this data is good only from $\xi = -2$ Å to $\xi = +0.5$ Å.

Figure 9, in red, shows the Jarzynski estimator for the free energy of set 1 (15+15 structures, pulling speed of 2 Å/ps). In green, we present the same results for set 2 (5+5 structures, pulling speed of 1 Å/ps). They both have been obtained by joining the free energies obtained by exponential averaging of work from Fig. 8. The $\Delta G^{\ddagger}$ values obtained are 7.6 kcal/mol for the Jarzynski estimator (set of 15+15 QM–MM structures and pulling speed of of 2 Å/ps) and 7.5 kcal/mol for the umbrella sampling calculations. We can conclude that the different pulling velocities do not change quantitatively the $\Delta G^{\ddagger}$ values obtained. Although our $\Delta G^{\ddagger}$ values are lower compared to the experimental ones, (8 kcal/mol approximately vs. 15 kcal/mol) due to flaws in our DFT description, the calculated entropic effect is negative, in agreement with the experimental value (−9.1 eu). Previous calculation of the entropic effect for this reaction in [62] have computed the wrong sign.

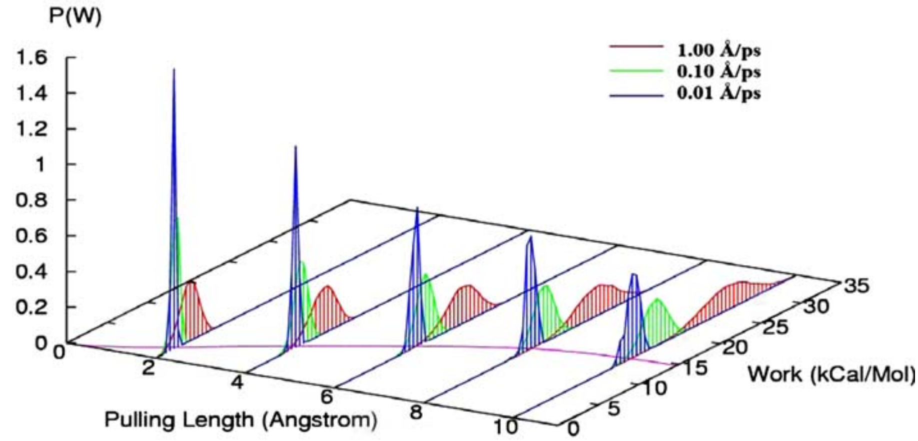

Fig. 5 Work distributions for different pulling rates

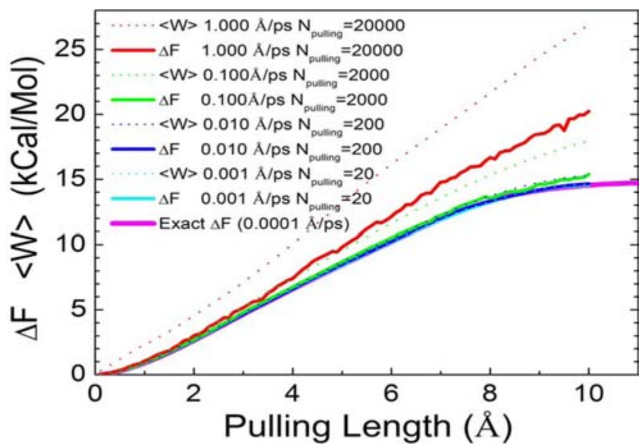

Fig. 6 Work averages and free energy differences calculated by Jarzynski's relationship for various pulling rates

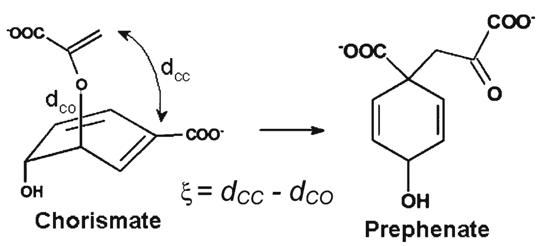

Fig. 7 Chorismate to prephenate conversion reaction

4.3 Ligand diffusion in globins

Mycobacterium tuberculosis, the causative agent of human tuberculosis, is responsible for more than a million deaths per year. In healthy individuals, the infection is contained by the immune system, which forces the bacteria into dormancy through a nitro-oxidative stress related mechanism. The toxic effects of NO can be reduced or even eliminated by the development of resistance mechanisms in microorganisms. One of such mechanisms consists in the oxidation of nitric oxide with heme bound O_2 to yield the innocuous nitrate ion [67]

$$Fe(II)O_2 + NO \rightarrow Fe(III) + NO_3.$$

M. tuberculosis encodes two small heme proteins [68], which belong to the family of the recently discovered truncated hemoglobins (TrHb) (for a recent review see Milani et al. [69]). The proximal HisF8 heme linked residue is conserved throughout the Hb and trHb families, and a distal TyrB10 is conserved in almost all the trHb family members sequenced to date.

Inspection of the available X-ray structures from several trHbs reveals that they host a protein tunnel/cavity system that connects the heme moiety with the exterior [70]. Recently it has been shown that these proteins can bind Xe atoms in the crystalline state, and that the Xe atoms map along the tunnel cavity system [71,72]. The tunnel, whose inner surface is mainly lined with non-polar residues, is about 20 Å long and is oriented perpendicular to the heme plane.

In a recent work we showed that NO reaction with coordinated oxygen is barrierless once NO is placed in the active site in *M. tuberculosis* trHb N, therefore once oxygen is bound, NO diffusion into the heme cavity is the rate limiting step [70].

In this section we use the JR to shed light on the ligand migration process along the tunnel/cavity system of *M. tuberculosis* trHbN. The chosen reaction coordinate λ was chosen as the iron–ligand distance. The force constant used was 200 kcal/molÅ^2. The pulling velocities used were 0.05 and 0.1 Å/ps. No significant differences in the ΔG profiles (less than 1 kcal/mol) were observed for both velocities for any given set of runs. To reconstruct the free energy profile for the tunnel the following sets of MSMD runs were performed: starting from equilibrated MD structures with $\lambda(t = 0)$ of 9, 13, and 17 Å, ten JR runs were performed in each direction (forward/exit and backward/entry) for each of the two pulling velocities. In cases where two overlapping profiles were obtained (from entry and exit sets), we confirmed that both of them matched.

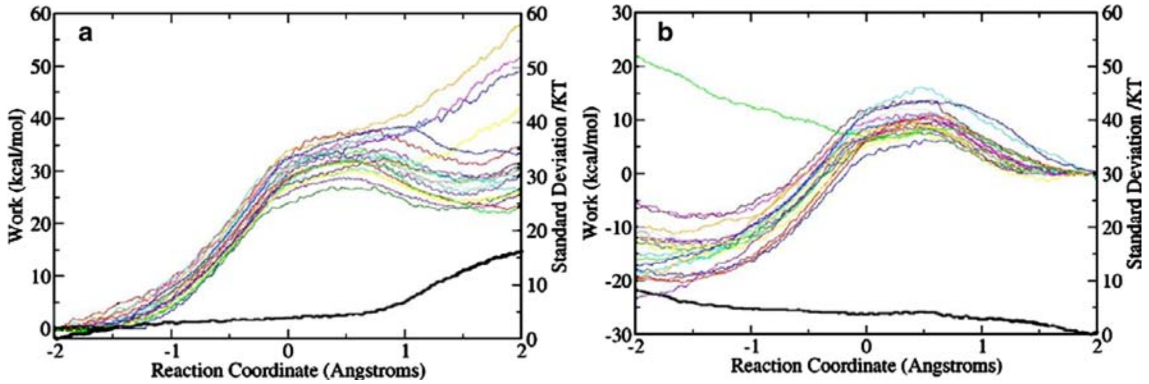

Fig. 8 **a** Chorismate to prephenate work for the 20 runs (*colored*) and the standard deviation (*thick black line*). **b** Prephenate to chorismate work for the 20 runs (*colored*) and the standard deviation (*thick black line*)

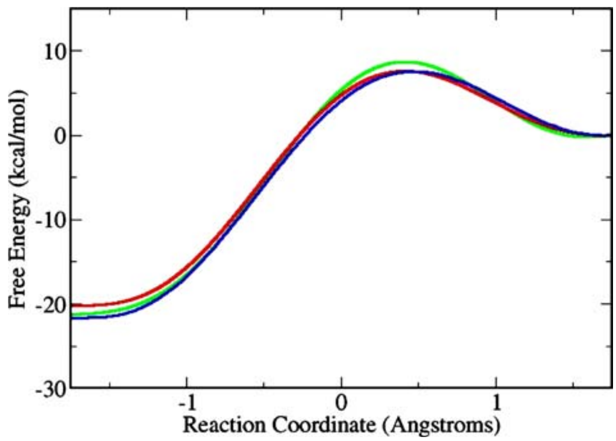

Fig. 9 Free energy profile from chorismate ($\xi \approx 1.75$ Å) to prephenate ($\xi \approx -1.75$ Å), calculated using Jarzynski's equality for set 1 (*red*), for set 2 (*green*) and umbrella sampling scheme (*blue*)

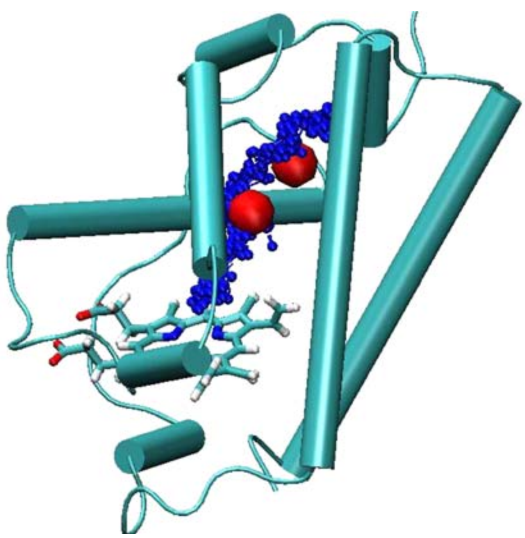

Fig. 10 *Blue balls* position of the ligand along the MSMD run (each point corresponds to each snapshot, taken at every picosecond). Protein: the protein coordinates are the mean position of the run. *Red balls* X-ray determined Xe atom docking positions

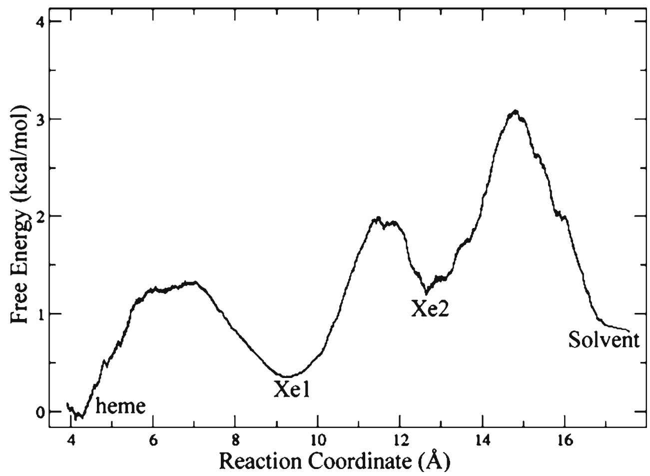

Fig. 11 Free energy profile (kcal/mol) along the tunnel (the reaction coordinate is defined as the Fe–N distance)

Analysis of the ligand position along the tunnel for several trajectories (Fig. 10) confirms that the ligand moves along the tunnel. The X-ray observed Xe binding sites match the trajectories described by the ligand along the simulations. The secondary docking sites corresponding to the free energy local minima in the free energy profile (Fig. 11), agree very well with the experimental Xe X-ray experiments. The simulation offers, as an added value, energetic information such as barrier heights and the possibility of obtaining microscopic insights about the interactions that govern the ligand diffusion process.

The free energy profiles and Xe X-ray derived data suggest that trHbs can accommodate several small neutral ligands. In this way the tunnels due to its apolar nature can significantly increase the solubility of molecules such as CO, O_2 or NO relative to the aqueous phase, acting as their concentrators [73,74].

5 Conclusions

The calculation of free energies of many processes has a long history within computational chemistry. With the introduction of the JR, and the recent formal and computational work associated with it, the field is ripe to witness a widespread use of this technique. As the ideas find their way into widely accessible software, we are bound to see new, unpredicted applications.

Acknowledgements We would like to thank Christopher Jarzynski and Tom Woolf for discussing many of the finer issues in non-equilibrium calculations with us. Part of this work was funded by the Department of Energy through grant DE-FG02-02ER45995. This work was partially supported by grants from Fundacion Antorchas, Universidad de Buenos Aires and ANPCYT. This work was partially supported by the National Computational Science Alliance (MCA05S010).

References

1. Chipot C, Pearlman DA (2002) Free energy calculations: the long and winding gilded road. Mol Simul 28(1–2):1–12
2. Jorgensen WL (2004) The many roles of computation in drug discovery. Science 303(5665):1813–1818
3. Ridder L et al (2002) Quantum mechanical/molecular mechanical free energy Simulations of the glutathione S-transferase (M1-1) reaction with phenanthrene 9,10-oxide. J Am Chem Soc 124(33):9926–9936
4. Shirts MR et al (2003) Extremely precise free energy calculations of amino acid side chain analogs: comparison of common molecular mechanics force fields for proteins. J Chem Phys 119(11):5740–5761
5. Jarzynski C (1997) Equilibrium free-energy differences from nonequilibrium measurements: a master-equation approach. Phys Rev E 56(5):5018–5035
6. Jarzynski C (1998) Equilibrium free energies from nonequilibrium processes. Acta Phys Pol B 29(6):1609–1622
7. Jarzynski C (2000) Hamiltonian derivation of a detailed fluctuation theorem. J Stat Phys 98(1–2):77–102
8. Jarzynski C (2001) How does a system respond when driven away from thermal equilibrium?. Proc Nat Acad Sci USA 98(7):3636–3638
9. Atilgan E, Sun SX (2004) Equilibrium free energy estimates based on nonequilibrium work relations and extended dynamics. J Chem Phys 121(21):10392–10400
10. Cohen EGD, Mauzerall D (2004) A note on the Jarzynski equality. J Stat Mech Theory Exp P07006[cond.mat/0406128]
11. Crooks GE (1998) Nonequilibrium measurements of free energy differences for microscopically reversible Markovian systems. J Stat Phys 90(5–6):1481–1487
12. Crooks GE (1999) Entropy production fluctuation theorem and the nonequilibrium work relation for free energy differences. Phys Rev E 60(3):2721–2726
13. Crooks GE (2000) Path-ensemble averages in systems driven far from equilibrium. Phys Rev E 61(3):2361–2366
14. Evans DJ (2003) A non-equilibrium free energy theorem for deterministic systems. Mol Phys 101(10):1551–1554
15. Evans DJ, Searles DJ (2002) The fluctuation theorem. Adv Phys 51(7):1529–1585
16. Gullingsrud JR, Braun R, Schulten K (1999) Reconstructing potentials of mean force through time series analysis of steered molecular dynamics simulations. J Comput Phys 151(1):190–211
17. Hummer G, Szabo A (2001) Free energy reconstruction from nonequilibrium single-molecule pulling experiments. Proc Nat Acad Sci USA 98(7):3658–3661
18. Hummer G, Szabo A (2003) Kinetics from nonequilibrium single-molecule pulling experiments. Biophys J 85(1):5–15
19. Jarzynski C (2004) Nonequilibrium work theorem for a system strongly coupled to a thermal environment. J Stat Mech Theory Exp P09005[Cond.mat/99121121]
20. Jou D, Casas-Vazquez J (2004) About some current frontiers of the second law. J Non-Equilib Thermodyn 29(4):345–357
21. Keller D, Swigon D, Bustamante C (2003) Relating single-molecule measurements to thermodynamics. Biophys J 84(2):733–738
22. Rickman JM, LeSar R (2002) Free-energy calculations in materials research. Ann Rev Mater Res 32:195–217
23. Ritort F (2004) Work and heat fluctuations in two-state systems: a trajectory thermodynamics formalism. J Stat Mech Theory Exp P10016[Cond.mat/0401311]
24. Ritort F, Bustamante C, Tinoco I (2002) A two-state kinetic model for the unfolding of single molecules by mechanical force. Proc Nat Acad Sci USA 99(21):13544–13548
25. Schurr JM, Fujimoto BS (2003) Equalities for the nonequilibrium work transferred from an external potential to a molecular system: analysis of single-molecule extension experiment. J Phys Chem B 107(50):14007–14019
26. Sun SX (2003) Equilibrium free energies from path sampling of nonequilibrium trajectories. J Chem Phys 118(13):5769–5775
27. Ytreberg FM, Zuckerman DM (2004) Single-ensemble nonequilibrium path-sampling estimates of free energy differences. J Chem Phys 120(23):10876–10879
28. Gore J, Ritort F, Bustamante C (2003) Bias and error in estimates of equilibrium free-energy differences from nonequilibrium measurements. Proc Nat Acad Sci USA 100(22):12564–12569
29. Hermans J (1991) Simple analysis of noise and hysteresis in (slow-growth) free-energy simulations. J Phys Chem 95(23):9029–9032
30. Hu H, Yun RH, Hermans J (2002) Reversibility of free energy simulations: slow growth may have a unique advantage (with a note on use of Ewald summation. Mol Simul 28(1–2):67–80
31. Hummer G (2001) Fast-growth thermodynamic integration: Error and efficiency analysis. J Chem Phys 114(17):7330–7337
32. Rodriguez-Gomez D, Darve E, Pohorille A (2004) Assessing the efficiency of free energy calculation methods. J Chem Phys 120(8):3563–3578
33. Rosso L et al (2002) On the use of the adiabatic molecular dynamics technique in the calculation of free energy profiles. J Chem Phys 116(11):4389–4402
34. Wu D, Kofke DA (2004) Model for small-sample bias of free-energy calculations applied to Gaussian-distributed nonequilibrium work measurements. J Chem Phys 121(18):8742–8747
35. Wu D, Kofke DA (2004) Asymmetric bias in free-energy perturbation measurements using two Hamiltonian-based models. Phys Rev E 70(6):066702-1–066702-11
36. Zuckerman DM, Woolf TB (2002) Overcoming finite-sampling errors in fast-switching free-energy estimates: extrapolative analysis of a molecular system. Chem Phys Lett 351(5–6):445–453
37. Zuckerman DM, Woolf TB (2002) Theory of a systematic computational error in free energy differences. Phys Rev Lett 89(18):180602
38. Zuckerman DM, Woolf TB (2004) Systematic finite-sampling inaccuracy in free energy differences and other nonlinear quantities. J Stat Phys 114(5–6):1303–1323
39. Isralewitz B et al (2001) Steered molecular dynamics investigations of protein function. J Mol Graph Model 19(1):13–25
40. Isralewitz B, Gao M, Schulten K (2001) Steered molecular dynamics and mechanical functions of proteins. Curr Opin Struct Biol 11(2):224–230
41. Bustamante C et al (2004) Mechanical processes in biochemistry. Annu Rev Biochem 73:705–748
42. Wang GM et al (2002) Experimental demonstration of violations of the second law of thermodynamics for small systems and short time scales. Phys Rev Lett 89(5):050601
43. Amaro R, Luthey-Schulten Z (2004) Molecular dynamics simulations of substrate channeling through an alpha-beta barrel protein. Chem Phys 307(2–3):147–155
44. Cascella M et al (2002) Multiple steering molecular dynamics applied to water exchange at alkali ions. J Phys Chem B 106(50):13027–13032
45. Cascella M, Raugei S, Carloni P (2004) Formamide hydrolysis investigated by multiple-steering ab initio molecular dynamics. J Phys Chem B 108(1):369–375

46. Hummer G (2002) Fast-growth thermodynamic integration: results for sodium ion hydration. Mol Simul 28(1–2):81–90
47. Li PC, Makarov DE (2003) Theoretical studies of the mechanical unfolding of the muscle protein titin: bridging the time-scale gap between simulation and experiment. J Chem Phys 119(17):9260–9268
48. Raugei S, Cascella M, Carloni P (2004) A proficient enzyme: insights on the mechanism of orotidine monophosphate decarboxylase from computer simulations. J Am Chem Soc 126(48):15730–15737
49. Vidossich P, Cascella M, Carloni P (2004) Dynamics and energetics of water permeation through the aquaporin channel. Proteins-Struct Funct Bioinformatics 55(4):924–931
50. Zwanzig RW (1954) High-temperature equation of state by a perturbation method. 1: nonpolar gases. J Chem Phys 22(8):1420–1426
51. Liu HY, Mark AE, vanGunsteren WF (1996) Estimating the relative free energy of different molecular states with respect to a single reference state. J Phys Chem 100(22):9485–9494
52. Oostenbrink C, van Gunsteren WF (2004) Free energies of binding of polychlorinated biphenyls to the estrogen receptor from a single simulation. Proteins-Struct Funct Genet 54(2):237–246
53. Okamoto Y (2004) Generalized-ensemble algorithms: enhanced sampling techniques for Monte Carlo and molecular dynamics simulations. J Mol Graph Model 22(5):425–439
54. Ponder J (2004) Tinker program. Available at http://dasher.wustl.edu/tinker/
55. Crespo A et al (2005) Multiple–steering QM-MM calculation of the free energy profile in chorismate mutase. J Am Chem Soc 127(19):6940–6941
56. Crespo A et al (2003) A DFT-based QM–MM approach designed for the treatment of large molecular systems: application to chorismate mutase. J Phys Chem B 107(49):13728–13736
57. Lee YS et al (2002) Reaction mechanism of chorismate mutase studied by the combined potentials of quantum mechanics and molecular mechanics. J Phys Chem B 106(46):12059–12065
58. Kast P et al (1997) Thermodynamics of the conversion of chorismate to prephenate: experimental results and theoretical predictions. J Phys Chem B 101(50):10976–10982
59. Woodcock HL et al (2003) Exploring the quantum mechanical/molecular mechanical replica path method: a pathway optimization of the chorismate to prephenate Claisen rearrangement catalyzed by chorismate mutase. Theor Chem Acc 109(3):140–148
60. Worthington SE, Roitberg AE, Krauss M (2001) An MD/QM study of the chorismate mutase-catalyzed Claisen rearrangement reaction. J Phys Chem B 105(29):7087–7095
61. Guimaraes CRW et al (2003) Contributions of conformational compression and preferential transition state stabilization to the rate enhancement by chorismate mutase. J Am Chem Soc 125(23):6892–6899
62. Marti S et al (2001) A hybrid potential reaction path and free energy study of the chorismate mutase reaction. J Am Chem Soc 123(8):1709–1712
63. Soler JM et al (2002) The SIESTA method for ab initio order-N materials simulation. J Phys Condens Matter 14(11):2745–2779
64. Chook YM et al (1994) The Monofunctional chorismate mutase from Bacillus-subtilis - structure determination of chorismate mutase and its complexes with a transition-state analog and prephenate, and implications for the mechanism of the enzymatic-reaction. J Mol Biol 240(5):476–500
65. Wang JM, Cieplak P, Kollman PA (2000) How well does a restrained electrostatic potential (RESP) model perform in calculating conformational energies of organic and biological molecules?. J Comput Chem 21(12):1049–1074
66. Torrie GM, Valleau JP (1977) Non-physical sampling distributions in Monte-Carlo free-energy estimation – umbrella sampling. J Comput Phys 23(2):187–199
67. MacMicking JD et al (1997) Identification of nitric oxide synthase as a protective locus against tuberculosis. Proc Nat Acad Sci USA 94(10):5243–5248
68. Couture M et al (1999) A cooperative oxygen-binding hemoglobin from Mycobacterium tuberculosis. Proc Nat Acad Sci USA 96(20):11223–11228
69. Milani M et al (2005) Structural bases for heme binding and diatomic ligand recognition in truncated hemoglobins. J Inorg Biochem 99(1):97–109
70. Crespo A et al (2005) Theoretical study of the truncated hemoglobin HbN: exploring the molecular basis of the NO detoxification mechanism. J Am Chem Soc 127(12):4433–4444
71. Milani M et al (2004) Cyanide binding to truncated hemoglobins: A crystallographic and kinetic study. Biochemistry 43(18):5213–5221
72. Milani M et al (2004) Heme-ligand tunneling in group I truncated hemoglobins. J Biol Chem 279(20):21520–21525
73. Samuni U et al (2003) Kinetic modulation in carbonmonoxy derivatives of truncated hemoglobins – the role of distal heme pocket residues and extended apolar tunnel. J Biol Chem 278(29):27241–27250
74. Dantsker D et al (2004) Viscosity-dependent relaxation significantly modulates the kinetics of CO recombination in the truncated hemoglobin TrHbN from Mycobacterium tuberculosis. J Biol Chem 279(37):38844–38853